



Evidence of calcium carbonates in coastal (Talos Dome and Ross Sea area) East Antarctica snow and firn: Environmental and climatic implications

M. Sala^{a,b,c,*}, B. Delmonte^a, M. Frezzotti^d, M. Proposito^d, C. Scarchilli^{d,e}, V. Maggi^a, G. Artioli^f, M. Dapiaggi^c, F. Marino^a, P.C. Ricci^g, G. De Giudici^h

^a Dipartimento di Scienze Ambientali (DISAT), Università degli Studi di Milano-Bicocca, P.zza della Scienza 1, 20126 Milano, Italy

^b Museo Nazionale Antartide, Via del Laterano 8, 53100 Siena, Italy

^c Dipartimento di Scienze della Terra "Ardito Desio", Università degli Studi di Milano, Via Botticelli 23, 20133 Milano, Italy

^d ENEA, Laboratorio Osservazioni Climatiche, C.R. Casaccia, Via Anguillarese 301, 00123 Roma, Italy

^e Dipartimento di Scienze della Terra, Università degli Studi di Siena, Via del Laterano 8, 53100 Siena, Italy

^f Dipartimento di Geoscienze, Università degli Studi di Padova, Via Giotto 1, 35137 Padova, Italy

^g Dipartimento di Fisica, Università degli Studi di Cagliari, Strada Provinciale Monserrato Sestu, 09042 Monserrato, Cagliari, Italy

^h Dipartimento di Scienze della Terra, Università degli Studi di Cagliari, Via Trentino 51, 09127 Cagliari, Italy

ARTICLE INFO

Article history:

Received 23 May 2007

Received in revised form 7 March 2008

Accepted 17 March 2008

Available online 9 April 2008

Editor: H. Elderfield

Keywords:

Antarctica
palaeoclimate
dust
mineralogy
atmospheric circulation

ABSTRACT

Micrometre-sized aeolian dust particles stored in Antarctic firn and ice layers are a useful tool for reconstructing climate and environmental changes in the past. The mineral content, particle concentration and chemical composition of *modern* dust in firn cores from the peripheral dome (Talos Dome) and coastal area of East Antarctica (Ross Sea sector) were investigated. During analyses there was a considerable decrease in microparticle concentrations within a few hours of ice sample melting, accompanied by a systematic increase in the concentration of calcium ions (Ca^{2+}) in solution. Based on mineralogical phase analyses, which reveal the presence of anhydrous and hydrous calcium carbonates such as calcite (CaCO_3), monohydrocalcite ($\text{CaCO}_3 \cdot \text{H}_2\text{O}$) and ikaite ($\text{CaCO}_3 \cdot 6\text{H}_2\text{O}$, hexahydrate calcium carbonate), the observed variations in concentrations are ascribed to the partial dissolution of the carbonate content of samples. Soluble carbonate compounds are thus primary aerosols included into the samples along with insoluble aluminosilicate minerals. We hypothesize hydrous carbonates may derive from the sea ice surface, where ikaite typically forms at the early stages of sea ice formation. Back trajectory calculations show that favourable events for air mass advection from the sea ice surface to Talos Dome are rare but likely to occur.

© 2008 Elsevier B.V. All rights reserved.

1. Introduction

The East Antarctic ice sheet is a natural archive of palaeoclimatic information, and long undisturbed sequences of data on environmental and atmospheric conditions can be obtained from ice and firn cores. Mineral dust records from polar ice cores have been studied extensively in order to reconstruct climate and atmospheric changes in the Late Quaternary at different timescales (Petit et al., 1999; Watanabe et al., 2003; EPICA Comm., 2004; NGRIP Project members, 2004). As a general observation, the net dust flux to the Antarctic was substantially greater during the Late Quaternary cold periods than during the warm interglacials (Petit et al., 1999; Delmonte et al., 2004; EPICA Comm., 2004).

Aeolian dust trapped in the firn and ice originates from the continental landmasses of the Southern Hemisphere. Physical and

chemical processes during airborne transport determine both particle size selection and mineralogical fractionation. The mineralogical composition and particle size variation in time is mainly related to changes in atmospheric circulation, the hydrological cycle and in the extent of deflation source areas (Maggi, 1997 and references therein). It is therefore extremely important to determine the geographic sources of mineral dust and their average composition in order to accurately interpret ice core glaciochemical data.

Mineralogical data obtained in the 1980s from the Vostok and EPICA – Dome C ice cores revealed the presence of clays as major mineral phases (i.e. illite, smectite, chlorite and kaolinite), and subordinate amounts of crystalline silica and feldspars (Gaudichet et al., 1986, 1988, 1992). More recent PIXE data (Proton Induced X-Ray Emission; Marino et al., 2004) and the $^{87}\text{Sr}/^{86}\text{Sr}$ versus $^{143}\text{Nd}/^{144}\text{Nd}$ isotopic signature of mineral particles seem to indicate that aeolian dust mainly originated in the southernmost part of South America during glacial periods, and that there was a substantial mixing of dust from different sources during the Holocene and stage 5.5 (Delmonte et al., 2007). In this context, geochemical analyses of Eastern Australian

* Corresponding author. Dipartimento di Scienze dell'Ambiente e del Territorio (DISAT), Università degli Studi di Milano-Bicocca, Piazza della Scienza 1, 20126 Milano, Italy. Tel.: +39 02 64482846 (Office); fax: +39 02 64482895.

E-mail address: marco.sala@unimib.it (M. Sala).

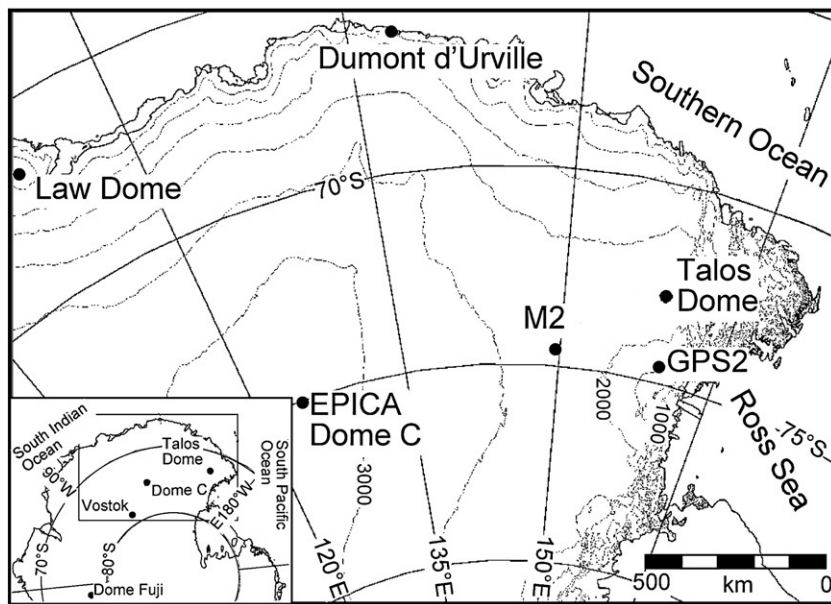


Fig. 1. Map of Antarctica showing the location of drilling sites mentioned in the text.

sediments suggest a contribution from this source to the Antarctic during warm periods (Marino et al., 2004; Revel-Rolland et al., 2006). In the case of drilling sites located in the Northern Victoria Land mountains, such as Hercules Nevé (Maggi and Petit, 1998), a contribution from local source areas must also be taken into account.

Our study mainly focuses on a shallow coastal firn core collected at Talos Dome (TDC core, 72°48'S, 159°06'E, 2316 m a.s.l., 53.7 m long, mean snow accumulation 80 kg/m² per year, 290 km from the Ross Sea and Southern Ocean) in the framework of the 2001 IT-ITASE (Italian-International Trans Antarctic Scientific Expedition) traverse (Frezzotti et al., 2004a) and on samples of two shallow coastal firn cores collected in the Ross Sea area, at M2 (74°48'S, 151°16'E; 2278 m a.s.l., 49.6 m long, mean acc. 15 kg/m² per year, 327 km from the Ross Sea) and GPS2 (74°38'S, 157°30'E; 1804 m a.s.l.; 43.6 m long, mean acc. 54 kg/m² per year, 167 km from the Ross Sea), during the 1998 IT-ITASE traverse (Frezzotti and Flora, 2002). The location of these sites is reported in Fig. 1. Climatological and glaciological conditions at the drilling sites are described by Stenni et al. (2002) and Frezzotti et al. (2004b, 2005).

In the present study we analysed mineral dust from shallow coastal Eastern Antarctic firn cores located in Northern Victoria Land, focusing specifically on the observed significant time-dependent decrease in the particle concentration of samples and on the increase in ionic Ca²⁺ in solution. This work aims to determine the mineralogy of dust in the Talos Dome and Ross Sea area.

2. Experimental

The dust particle concentration and size distribution, ion chemistry, mineralogical phase composition and molecular stretching were obtained by means of four independent analytical methods selected for their ability to investigate the small amount of material trapped in firn samples. Different specimens of the same shallow cores were employed for each analysis.

2.1. Sample preparation

The shallow firn cores were drilled using an electromechanical drilling system; cores were cut into sections about 50 cm long and stored in polyethylene bags at freezing temperature.

The Talos Dome (TDC) firn core was sampled every 12–15 cm for all measurements, which are therefore deemed to be representative of

annual or multi-annual deposition. In-situ Raman spectroscopy, applied only on the TDC core, required sub-sampling into small parallelepipeds measuring 3.5×1×1 cm. M2 and GPS2 samples were cut like those of Talos Dome for dust, chemistry and diffraction analyses. Sampling was performed in a cold room ($T < -15$ °C) at the Environmental Science Department of the University of Milano-Bicocca. Firn sample surfaces were decontaminated under laminar flow bench in the cold room and then in a class 1000 clean room using a ceramic knife to cut away the external portions of samples. Decontamination of samples is crucial when dealing with firn and ice from East Antarctica, where dust concentrations are very low.

Firn core samples were selected according to the availability of the core, taking into account the variability of the accumulation rate along the cores and the peculiarity of the analytical techniques used. This work focuses on two different sets of samples:

(Set I): 13 samples from the TDC core, 4 from GPS2 core and 4 from M2 core (Table 1) were cut, melted and analysed for dust concentration

Table 1

TDC, GPS2 and M2 firn samples (Set I) addressed for dust concentration, chemical ions concentration and mineral phase investigation

Sample	Dust concentration	Chemistry	XRPD
TDC 17B	X	X	Integrated sample
TDC 25B	X	X	
TDC 27B	X	X	
TDC 34B	X	X	
TDC 39B	X	X	
TDC 41B	X	X	
TDC 46B	X	X	
TDC 50B	X	X	
TDC 53B	X	X	
TDC 55B	X	X	
TDC 81A1	X	X	
TDC 81A2	X	X	
GPS2 10B	X	X	Integrated sample
GPS2 14A	X	X	
GPS2 43A	X	X	
GPS2 47	X	X	
M2 9A	X	X	Integrated sample
M2 11B	X	X	
M2 40A	X	X	
M2 49A	X	X	

and size distribution, chemical ions concentration and powder diffraction analysis. Dust and chemical analyses were performed on all samples, while some integrated samples (Fig. 2a) were prepared for X-Ray Powder Diffraction (XRPD) through filtration immediately after melting on a Nuclepore polycarbonate membrane. This step is necessary because of the very low amount of dust of the samples.

(Set II): After preliminary investigation on Set I of samples we focused on the first 30 m of the Talos Dome (TDC) firn core. The TDC firn core was sub-sampled in 250 sections for dust analysis and 40 samples for chemical investigation. TDC samples dedicated to Raman spectroscopy were chosen according to the relative decrease in dust particle concentration (soluble fraction disappearing 24 h after melting) along the dust record (Fig. 2b).

Dust concentration and chemical measurements were performed in a class 1000 clean room respectively at the Environmental Science Department – University of Milano-Bicocca and at the Environment, Global Change and Sustainable Development Department – ENEA C.R. Casaccia (Rome). Diffraction patterns were collected at the Earth Science Department – University of Milan and in-situ Raman spectra were obtained at the Physics Department – University of Cagliari.

2.2. Chemistry: evaluation of anion and cation contents

Total ionic concentrations were measured both for Set I and Set II at melting time (t_0) and after 24 h (t_{24}); samples were melted at room temperature in a clean room and analysed using a Dionex Chromatography System (DX500 Series). The cation channel was equipped with a CS12A (4 mm) analytical column, a CAES (Cation Atlas Electrolytic Suppressor) suppressor device, and an MSA isocratic solution (20 mM) as eluent. The anion channel was equipped with an AS11HC (2 mm) analytical column, an ASRS-ULTRA II (2 mm) suppressor device, and a NaOH gradient solution as eluent. The ion chromatography system was very stable during runs, and the analytical error for each of the ionic species was less than 10%. Before IC injection all the sample aliquots analysed were filtered through a pore size of 0.45 μm (Millipore MILLEX – HA). A first set (Set I) of samples (Tables 1 and 2), was chemically analysed for anion, cation and dust concentrations immediately after melting (t_0) and at different time intervals (1, 3, 5 and 8 h after melting) until a maximum of 11 h. Ca^{2+} concentration on the Set II of samples were investigated at t_0 and 24 h after melting (t_{24}); some samples were re-analysed after 48 h, but no changes in Ca^{2+} concentrations were observed. Sample pH was also measured at $\sim t_0$ following IUPAC recommendations (Durst et al., 1994).

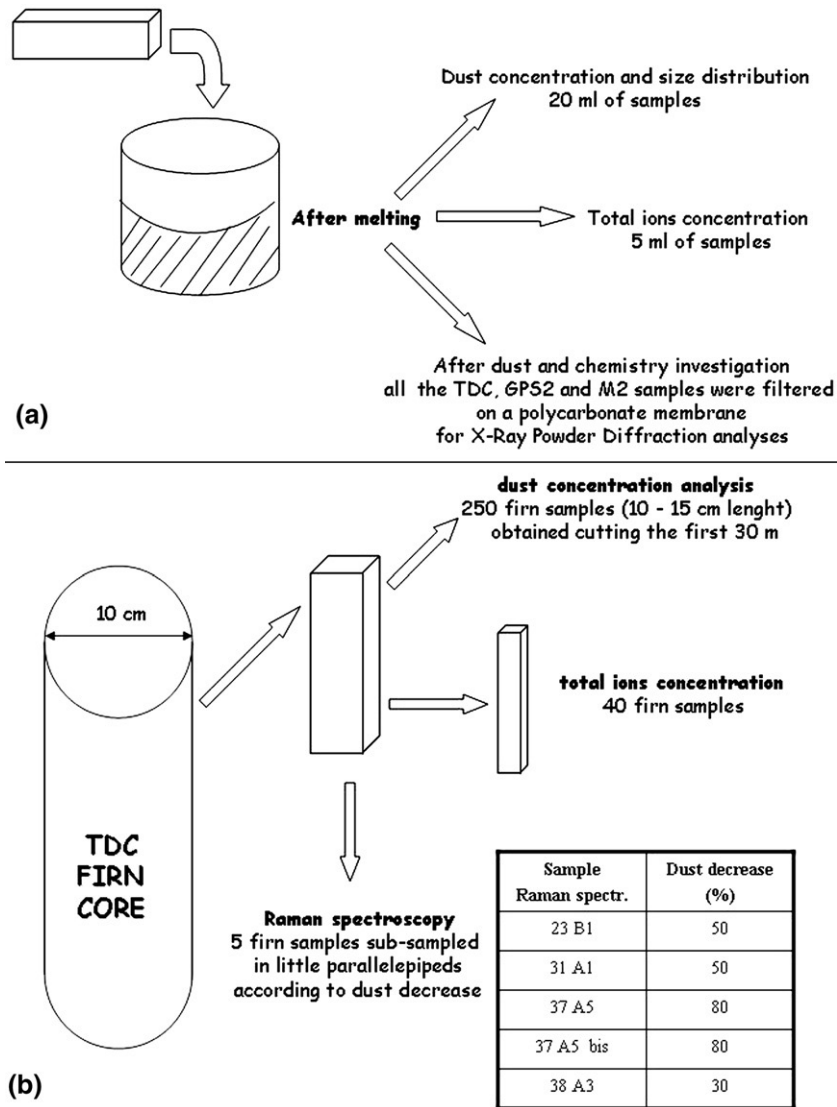


Fig. 2. (a) Set I samples: preparation and subdivision in aliquots for dust, chemistry and mineralogical investigation; (b) TDC core sampling: 250 firn samples were addressed for dust concentration and size distribution analysis and 40 samples for chemical ions investigation. According to the dust mass decrease (see table in the figure) and the availability of the core 5 firn samples were sub-sampled in little parallelepipeds for Raman spectroscopy.

Table 2
Variability of dust (ppb) and Ca^{2+} (10^{-8} mol/l) concentrations versus depth/time in firn samples from the considered sites

Sample	Depth (m)	Age	Dust concentration (ppb)				Ca^{2+} concentration (10^{-8} mol/l)			
			t_0	t_{max}	$t_0 - t_{\text{max}}$	T_{max} (time after t_0) (h)	t_0	t_{max}	$t_{\text{max}} - t_0$	T_{max} (time after t_0)
TDC 17B	13.88	1938	54.2	48.1	6.0	(3)	8.75	38.25	29.5	(11 h)
TDC 25B	19.39	1903	27.3	18.1	9.2	(6)	6.5	15.25	8.75	(11 h)
TDC 27B	21.26	1890	37.7	29.9	7.8	(1)	6.5	9.75	3.25	(11 h)
TDC 34B	26.25	1852	42.6	12.0	30.6	(3)	5.5	10.75	5.25	(11 h)
TDC 39B	29.58	1823	44.6	28.2	16.4	(3)	10.75	19	8.25	(11 h)
TDC 41B	30.91	1809	25.1	10.0	15.1	(6)	4.5	16	11.5	(8 h30')
TDC 44B	32.85	1794	54.9	23.4	31.5	(6)	10.25	25	14.75	(11 h)
TDC 46B	34.20	1782	25.8	12.6	13.2	(6)	5.5	10	4.5	(11 h)
TDC 50B	36.75	1755	22.8	11.5	11.3	(3)	6.75	17.5	10.75	(11 h)
TDC 53B	38.46	1739	26.3	14.8	11.5	(3)	7.5	15.75	8.25	(11 h)
TDC 55B	39.51	1725	54.0	31.9	22.1	(6)	10	15.5	5.5	(10 h)
TDC 81A1	52.48	1580	44.8	17.9	26.9	(6)	12	32.75	20.75	(8 h)
TDC 81A2	52.72	1578	45.6	17.7	27.9	(6)	5.5	19.25	13.75	(10 h30')
M2 9A	6.73		107	17	90	(6)	15	47.5	32.5	(11 h)
M2 11B	9.18		77	39	38	(3)	10	17.5	7.5	(11 h)
GPS2 10B	6.12		70	29	41	(6)	15	35	20	(11 h)
GPS2 43A	29.60		52	36	16	(6)	17.5	30	12.5	(11 h)

T_{max} represents the time elapsed after t_0 . M2 and GPS2 dating is in progress.

2.3. Particle concentration and size distribution of aeolian mineral dust

Firn samples were melted at room temperature in clean room under laminar flow bench. A Beckman Counter Multisizer III was used to measure total dust volume concentrations and particle size distributions following the procedure described in Delmonte et al. (2002). The instrument was equipped with a 50 μm orifice to measure particles from 1 μm to about 30 μm in size. The measured dust volume is obtained (Delmonte et al., 2002) between the first channel of measure and the first zero counts of the lognormal volume–size distribution, which is around 5 μm for inner Antarctica. The 1–5 μm size interval is typical of long-range transport. Accordingly, in the present work we also refer to the dust volume and mass (i.e. 10^{-9} g/g or ppb) of samples within the same interval. Although larger particles are rare (numerically less than 2%), they are sporadically present in samples and can account for a significant amount of volume. We did not consider this large-particle fraction because we could not guarantee the complete decontamination of the very delicate firn samples.

Of the Set I of samples chosen for chemical and dust analyses, four TDC samples (41 B–55 B–81 A1–81 AII) were analysed approximately every hour in order to observe in detail the decrease in dust concentration and size distribution; all other samples were analysed every 3–5 h. After these preliminary analyses, the first 30 m of the TDC core (Set II) were analysed at t_0 and after 24 h (each measurement repeated three times). Samples were continuously stirred mechanically, except in the short interval of time required for analysis (50 s per analysis, repeated three times).

2.4. X-Ray Powder Diffraction (XRPD): mineralogical characterization of Antarctic dust

Firn samples from TDC, GPS2 and M2 firn cores (Set I) were filtered immediately after melting, and then analysed by X-Ray Powder Diffraction (XRPD) technique. Firn samples were deposited on polycarbonate membranes immediately after melting and were then analysed by means of diffraction techniques in order to characterize the mineral phase composition of aeolian dust trapped in firn and ice cores. Particle contents were deposited on a Nuclepore track-etch membrane using a dedicated filtering device (Marino et al., 2004, in press; Dapiaggi et al., 2007). Since the filtered contents did not meet the statistical requirements for performing standard XRPD analysis, we used the very sensitive PANalytical X'pert PRO diffractometer equipped with a multi-channel X'celerator detector, and adopted a special grazing incidence procedure developed to increase sensitivity on thin

diluted samples (Dapiaggi et al., 2007). Analyses were performed in parallel beam geometry, in $\theta/2\theta$ scan (Dapiaggi et al., 2007). Each pattern was collected in about 4 h (with angular range 5–70°2 θ , steps of about 0.016°2 θ , and a counting time of 450 s/step).

2.5. In-situ Raman spectroscopy on Antarctic firn cores (Talos Dome core, TDC)

Samples from TDC firn core (Set II) were analysed in Raman spectroscopy; each specimen was sub-sampled into small parallelepipeds measuring 3.5×1×1 cm. Firn samples were collected at a depth of 18.20 m, 23.59 m, 28.00 m, 28.10 m and 28.62 m. In this work in-situ Raman spectroscopy was used to characterize the symmetric stretching of the carbonate group trapped in the Talos Dome firn core. Raman measurements were performed on adjacent core sections at the same depth used for dust and chemical analysis, in order to evaluate effective presence of carbonates and/or other compounds directly in the firn. Analyses were performed directly on the solid samples inserted in a Peltier cooling cell, coupled with a PVC box with a quartz window, and maintained at $T=263$ K during measurement. A vacuum of about 1300 Pa was created inside the sample box in order to avoid condensation of humidity on the surface of the ice. Raman scattering measurements were carried out in backscattering geometry using the 514.5 nm line of an argon-ion laser. Analyses were performed using a triple spectrometer Jobin-Yvonne Dilor integrated system with a spectral resolution of about 1/cm. Spectra were recorded in the Stokes region by a 1200 grooves 1/mm grating monochromator and a charge-coupled (CCD) detection system.

Dispersions of about 10, 50 and 200 μg of calcite trapped in 50 ml of frozen ultrapure water (MilliQ) were prepared as standards and analysed for precise calibration of the symmetric stretching peaks of CO_3^{2-} and OH^- and for the water bending mode (Minceva-Sukarova et al., 1984; Clarkson et al., 1992). Each spectrum was collected for about 1 h, and three replicated measurements were made in the 300–2200 1/cm spectral range. In-situ Raman spectroscopy was applied to ice samples from Dome Fuji (Ohno et al., 2005), and has been applied to firn samples from Talos Dome for the first time in this work. The main challenges are the difficult beam focus on samples, the very small quantity of particles and the inhomogeneous dispersion of carbonates in the cores (confirmed during dust particles and mineral standard analyses). We analysed a total of 25 little firn pieces: some specimens were melted during set-up, but we successfully collected ikaite and calcium carbonates spectra from 10 parallelepiped firn samples. Moreover, many spectra were obtained from different points of the same sample (TDC 37A-5 and TDC 37A-5 bis firn samples are an example of this analytical strategy) to check for sampling and

measurement statistics, and to determine instrument sensitivity as a function of particle concentration and dispersion.

3. Results

3.1. Preliminary correlation between the decrease in dust and increase in calcium (Ca^{2+}) concentrations

The majority of samples from Set I, selected for particle concentration and size distribution analyses and for parallel measurements of major anions (Cl^- , NO_3^- , SO_4^{2-}) and cations (Na^+ , K^+ , Mg^{2+} , Ca^{2+}), showed a consistent decrease in particle concentrations over time, starting 30–60 min after melting (t_0). The decrease was very pronounced in the first 3–4 h (Fig. 3a), but about 12 h after t_0 all samples showed stable dust concentrations identical to those measured 24 h after melting (t_{24}). The net dust loss, on average $\sim 45\%$ of the initial concentration at t_0 , was highly variable from sample to sample (0 to $\sim 80\%$). The dust mass was calculated from the measured dust volume, assuming a mean density of 2.5 g/cm^3 (the average density of minerals from the upper continental crust).

Up to 11–12 h after melting also reveal a systematic increase in Ca^{2+} in solution (Fig. 3a) with no significant variations in the concentration

of other measurable ions (Fig. 3b). Ca^{2+} concentrations can be considered stable on average about 11 h after t_0 . On average, Ca^{2+} increased by $12.5 \times 10^{-8} \text{ mol/l}$ in all samples analysed (Table 2), ranging from 3.25×10^{-8} (TDC 27B) to 32.5×10^{-8} (M2 9A) mol/l . The decrease in dust mass and increase in Ca^{2+} in solution suggest that relatively rapid dissolution processes occur. The weight ratio of Ca^{2+} to sodium (Na^+) is at least one order of magnitude greater than that of SMOW (i.e. Standard Mean Ocean Water) (Table 3) and indicates a clear enrichment in Ca^{2+} in all samples. The weight ratio of SO_4^{2-} to Na^+ indicates that there is also a consistent enrichment in SO_4^{2-} with respect to SMOW, which can be attributed to the significant S-rich contribution of marine biogenic emissions. Comparison between Na^+ and other sea water ions (chloride, magnesium) reveals no significant depletion of Na^+ with respect to SMOW. The pH of all samples was acidic (between 5.3 and 5.6) at melting time and increased by about 0.3–0.5 after 24 h.

3.2. Large amounts of calcite in firn cores

This study provides the first X-Ray Powder Diffraction data on extremely low amounts of mineral dust extracted from Antarctic firn (Dapiaggi et al., 2007). However, the mineralogical composition of

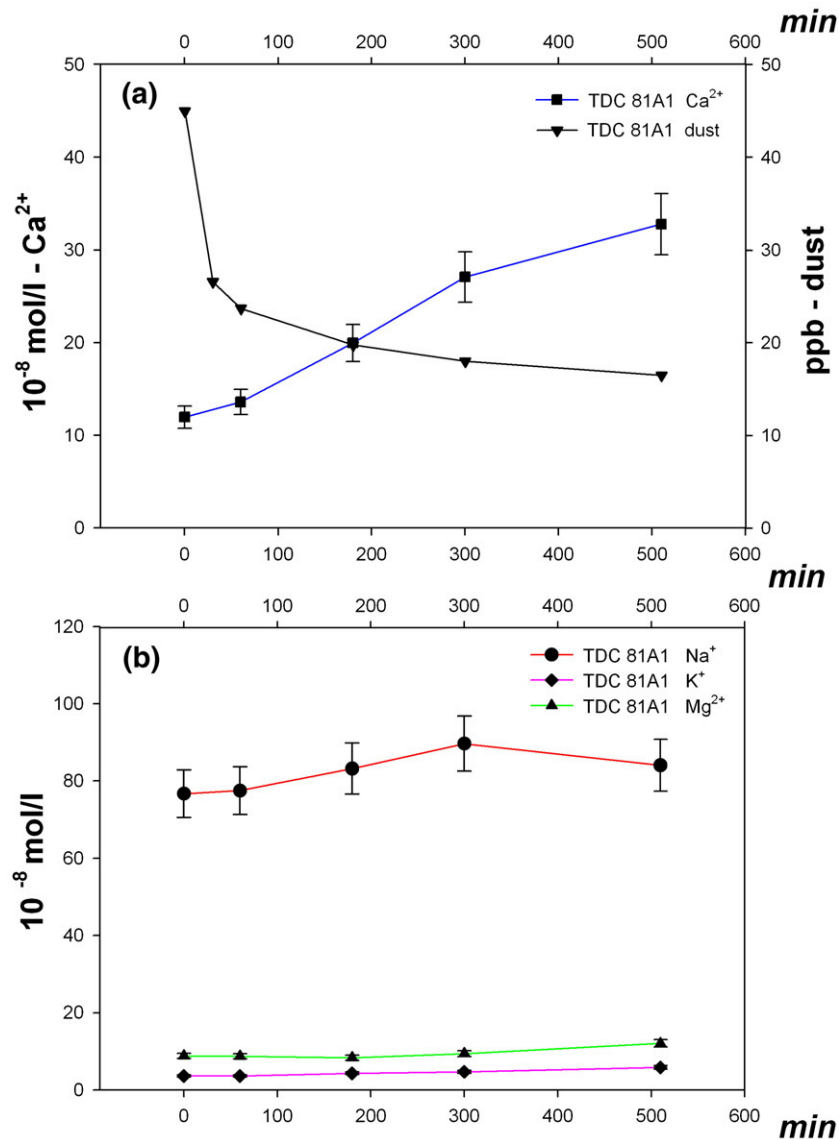


Fig. 3. (a) The increase in Ca^{2+} (10^{-8} mol/l) and decrease in dust (ppb) concentrations in the 8 h interval after sample melting. (b) No significant variations are visible in the other cation measurements during the 8 h interval after samples melting.

Table 3

Weight ratios of ions in firn samples from the studied sites showing the Ca^{2+} and SO_4^{2-} excess with respect to SMOW (i.e. Standard Mean Ocean Water)

Sample	$\text{Ca}^{2+}/\text{Na}^+$	$\text{SO}_4^{2-}/\text{Na}^+$
SMOW	0.038	0.252
TDC 17B	0.438	1.632
TDC 25B	0.290	3.278
TDC 27B	0.179	2.701
TDC 34B	0.203	4.065
TDC 39B	0.252	1.635
TDC 41B	0.321	5.787
TDC 44B	0.248	1.747
TDC 46B	0.161	2.863
TDC 50B	0.274	1.524
TDC 53B	0.253	3.813
TDC 55B	0.187	2.392
TDC 81A1	0.439	2.657
TDC 81A2	0.407	5.800
M2 9A	0.400	2.912
M2 11B	0.223	2.394
GPS2 10B	0.384	3.190
GPS2 43A	0.151	1.148

dust particles was previously investigated by means of single crystal technique (Gaudichet et al., 1986, 1988, 1992; Briat et al., 1982).

Most XRPD spectra obtained in this work show the presence of calcite as well as quartz, K-feldspars and clays such as illite, kaolinite and smectite. These results agree with the pioneering mineralogical investigation of ice samples from Dome C and Vostok (Briat et al., 1982; Gaudichet et al., 1986) showing clay as the dominant mineral phase (~40% of the total number of particles) with subordinate feldspars and crystalline silica (about 15% for each phase). Illite represents ~60% of all clays in Vostok ice (Gaudichet et al., 1992), whereas smectite, chlorite and kaolinite are less abundant.

According to particle counter estimates, the total amount of dust mass deposited on the filters was extremely low (from ~5 μg to a maximum of 30 μg of mineral materials). Four XRPD measurements are shown in Fig. 4 as examples. All samples show measurable diffraction peaks, and using appropriate calibration curves on standard mineral phases (Dapiaggi et al., 2007) some quantitative estimates can be made. Estimation of each mineral phase is possibly down to 1–2 μg (in terms of absolute quantities present on the filter).

Since the amount of minerals trapped in Antarctic firn is extremely low, some diffraction patterns only show one clear peak and apparently no other mineral phases. In the case of sample TDC 56A1 only the calcite diffraction peak is visible above the background.

3.3. Talos Dome dust record: two centuries of climatic variations

Dust concentration and size distribution were measured on the first 30 m of the TDC core (Set II), corresponding to the time period from 1814 to 2001 A.D. Analysis of snow radar and volcanic peaks between the TDC and the TD cores (Stenni et al., 2002) shows that internal radar layering is continuous and horizontal and depth of volcanic peaks are consistent with different drilling age (1996–2001 A.D.) between the two cores (Frezzotti et al., 2004a, 2007). Therefore, we established the chronology of the TDC core by adopting the 7-year running mean accumulation rate at TD (Stenni et al., 2002; Frezzotti et al., 2007). Dating accuracy is estimated to be ± 3.5 yr (Frezzotti et al., 2007).

Dust was measured at t_0 and t_{24} . The concentration at t_0 represents the total mass of the samples measured immediately after melting, whereas the dust concentration at t_{24} likely reflects the contribution from the residual insoluble fraction, which probably consists of aluminosilicates (see Fig. 5a). The dust mass was calculated from the measured dust volume assuming an average density of 2.5 g/cm^3 ; although this assumption is valid for aeolian dust from the interior of Antarctica (e.g. Delmonte et al., 2002), it could be questioned for our samples because aluminosilicates are mixed with light salts having a much lower density (e.g. 1.77 g/cm^3 for ikaite; Pauly, 1963 and 2.38 g/cm^3 for monohydrocalcite; Dahl and Buchard, 2006). The dust mass levels of Fig. 5a could therefore be overestimated by a maximum factor of 1.4. Nonetheless, the average dust concentration over the last two centuries was estimated to be 31(± 19) ppb immediately after melting and 17(± 9) ppb after 24 h.

These insoluble dust levels measured in firn from TDC are close to those in firn from Vostok and EPICA-Dome C and in other ice cores from the East Antarctic interior (15–20 ppb, 0.5 mg/m^2 per year, according to Delmonte et al., 2005) calculated for the Early and Middle Holocene (2 to 10 kyr B.P.) where data are available. The volume (mass) size distribution of insoluble dust at TDC is also similar to that of deep ice samples from the plateau, i.e. log-normally distributed around a mean (mass) mode of ca. 2 μm , with the sporadic occurrence of larger particles.

The difference between the dust mass at melting time (t_0) and after 24 h represents the fraction of soluble microparticles, which is plotted

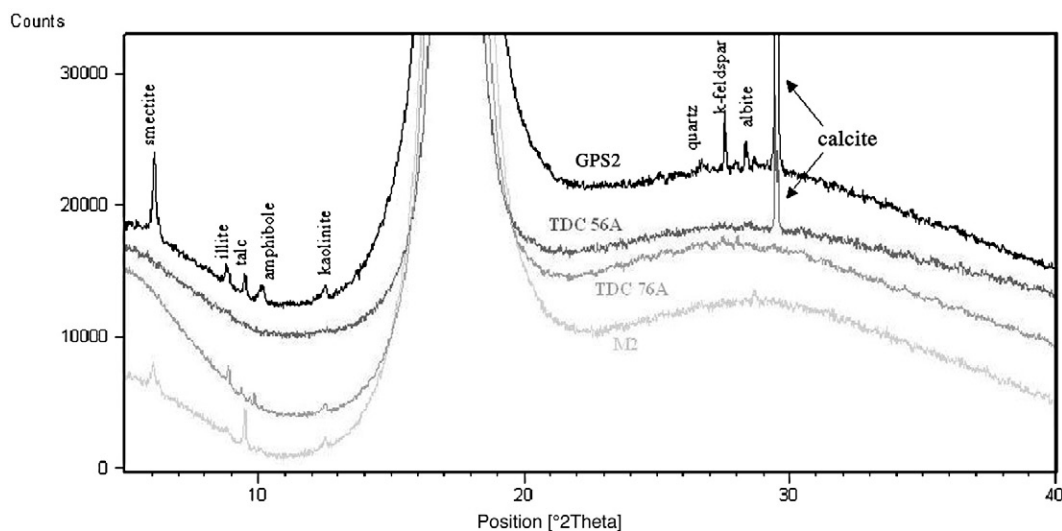


Fig. 4. XRPD spectra of 4 samples filtered immediately after melting. Two samples are from the TDC core, one from the M2 core, and another from the GPS2 core. Since the amount of minerals trapped in firn is extremely low and quantification of mineral phases is possible down to 1–2 μg , some diffraction patterns (e.g. TDC 56A1) show only the main peak of the major mineral phase above background.

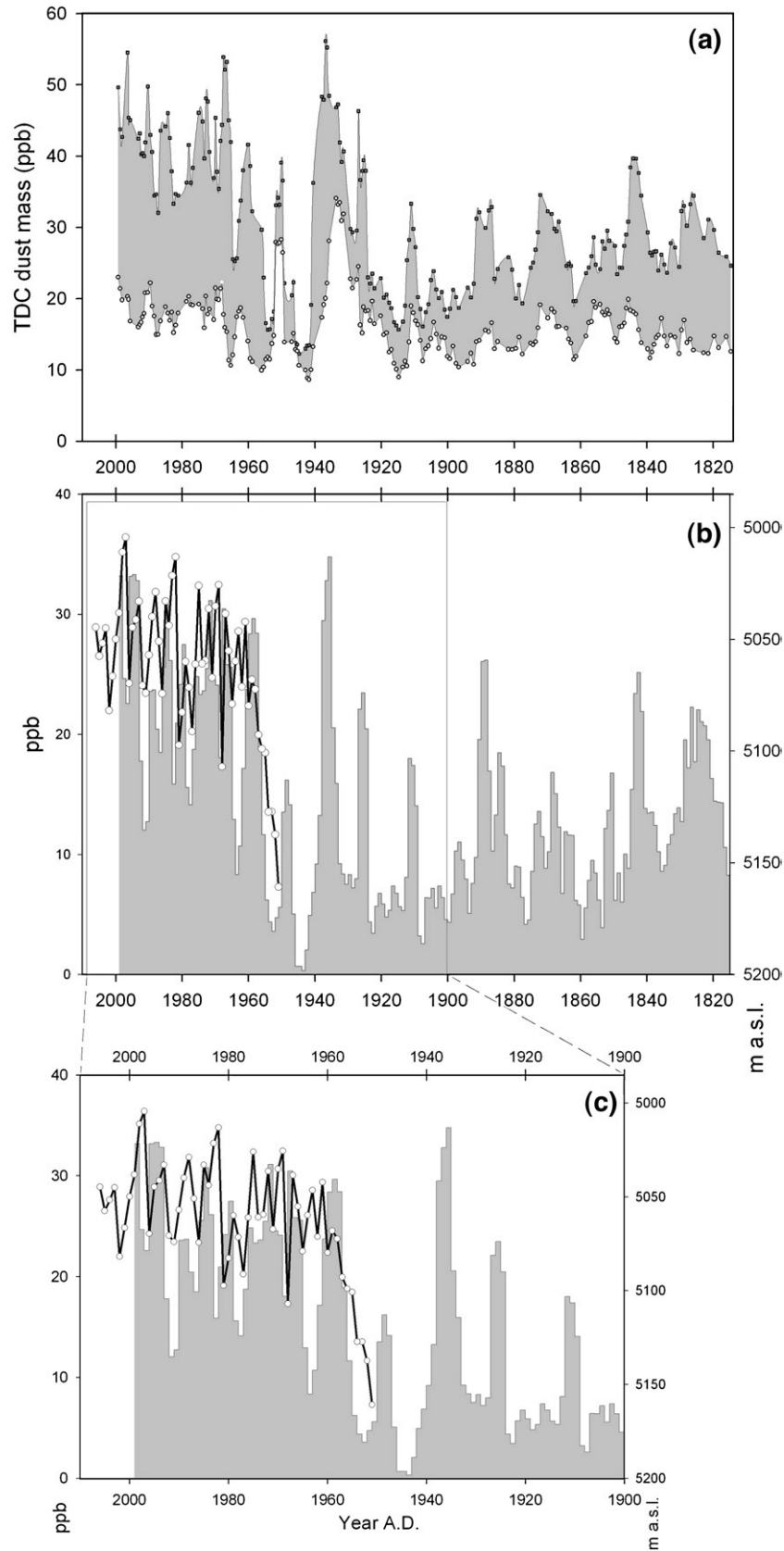


Fig. 5. Dust record in the first 30 m of the TDC1 firn core (TDC1 chronology, see text). The upper line represents total (soluble and insoluble) dust concentrations measured immediately after melting (t_0), whereas the bottom line represents dust concentrations 24 h after melting (t_{24}), which are likely related to the insoluble (aluminosilicate) fraction. The difference between the two concentration records is reported in b (grey line) as concentration (ppb). The black line with open circles shows the annual average altitude (m a.s.l.) of the 500 mbar geopotential height in the 60–70°S, 150–200°E sector (from NCEP/NCAR data re-analysis). c shows dust and geopotential variability during the last 100 yr.

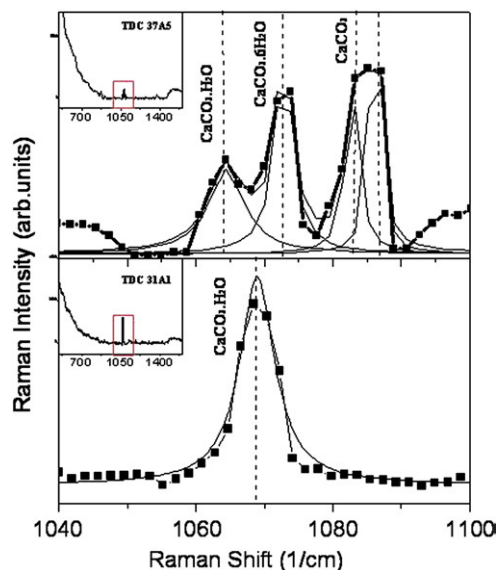


Fig. 6. Raman spectra of two TDC firn samples providing evidence for the presence of hydrous calcium carbonate phases (samples TDC 31A1 and TDC 37A5). The peaks are fitted by means of Lorentzian equations. The top spectrum shows the characteristic stretching mode of monohydrate, hexahydrate and anhydrous calcite at 1064 1/cm, 1073 1/cm and 1085 1/cm respectively, while the bottom spectrum shows only monohydrate calcium carbonate ($\text{CaCO}_3 \cdot \text{H}_2\text{O}$) stretching at 1068 1/cm.

in Fig. 5b and c as dust mass (ppb). This soluble fraction on average represents about 43% of the total mass at t_0 , but it is highly variable in time (from less than 10% to more than 70%). Interestingly, any significant correlation exists between the insoluble (t_{24}) and soluble (t_0 minus t_{24}) dust masses. Along the TDC profile 40 samples (Set II) were selected for parallel calcium analyses performed at t_0 and t_{24} . On average, Ca^{2+} contents increased when dust concentrations decreased by about 17% and 43% respectively, but these proportions are slightly variable between the pre-1940 part of the record (17% and 42% respectively, 16 samples), the 1940–1960 period (14% and 37% respectively, 14 samples) and the most recent part of the record extending from 1960 to 1990 (22% and 50% respectively, 10 samples).

3.4. Occurrence of ikaite in Antarctic firn cores and climatic implications

Raman scattering analyses were performed directly on firn samples because this technique is very sensitive to ultra-diluted concentrations. Furthermore, the carbonate mineral phase can be readily identified as the shift in the carbonate stretching peak is directly related to the structural environment of the carbonate group in the anhydrous and hydrated forms. Raman scattering analyses were carried out under controlled atmospheric and temperature conditions in order to avoid dehydration of hydrous calcium carbonate forms. Indeed, both hexahydrate (named ikaite) and monohydrate calcite are very unstable at temperatures above 273 K.

The Raman spectra from two TDC firn samples (TDC 31A1 and TDC 37A5), fitted by a series of Lorentzian peaks, are shown as an example in Fig. 6; similar results were obtained on eight other TDC parallelepiped samples. The absence of calcium carbonate stretching during data collection is related to the non-homogeneous dispersion of particles and to very low concentrations (lower than the Raman detection limit) in the core. The characteristic stretching of monohydrate, hexahydrate and anhydrous calcite can be clearly observed at 1064 1/cm, 1073 1/cm and 1085 1/cm in sample TDC 37A5, in agreement with the results obtained by Tlili et al. (2001) using a micro-Raman technique. Only the monohydrate $\text{CaCO}_3 \cdot \text{H}_2\text{O}$ stretching peak at 1068 1/cm is visible in sample TDC 31A1. We observed a small shift in the symmetric stretching of monohydrocalcite, in agreement with the results of Coleyshaw et al. (2003). Raman analysis of TDC firn samples therefore provides direct evidence for the presence of ikaite and monohydrate calcium carbonate in this core.

4. Discussion

4.1. The dust volume decrease: dehydration and solubilization of calcium carbonates

Firn samples from three coastal East Antarctic sites located in the Ross Sea and Talos Dome area show a considerable decline in insoluble microparticle concentrations a few hours after melting, with systematic increases in Ca^{2+} in solution but with no significant variability in the other measurable ions (Na^+ , K^+ , Mg^{2+} , Cl^- , SO_4^{2-} and NO_3^-). X-Ray Powder Diffraction analysis of dust particles extracted by filtering immediately after melting reveals the presence of CaCO_3 (calcite) along with

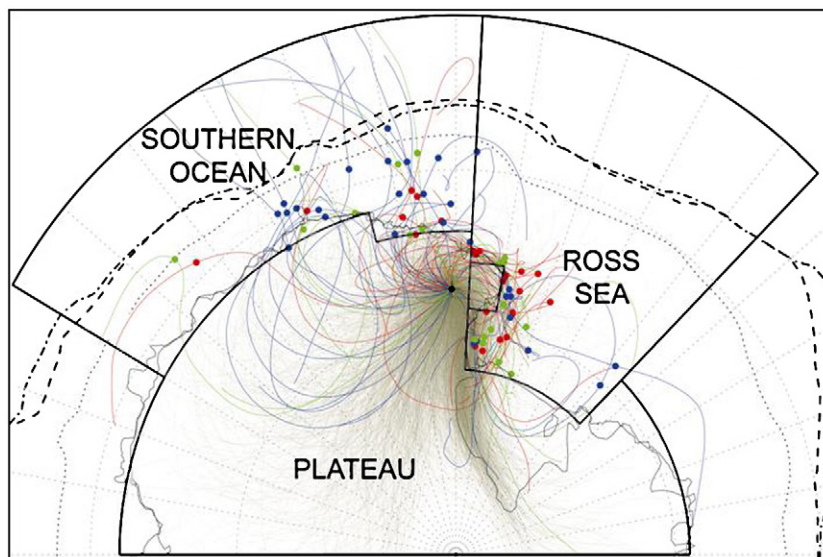


Fig. 7. Two-day back trajectories starting 1000 m above Talos Dome from 01/02/1990 to 01/02/2002 (grey lines). Trajectories fulfilling threshold conditions (Ice Concentration > 0.5%, Wind Speed > 8 m/s, see text) are marked in red (fall), blue (winter) and green (spring); the filled circles (same colours) show upload locations. The seasonal average of maximum sea ice coverage (ECMWF ERA 40 data) is shown as dotted (fall), dashed (winter) and dot-dashed (spring) lines. The different sectors are marked with black lines and labels (Inland Plateau, Ross Sea, Southern Ocean).

insoluble aluminosilicates. In-situ Raman scattering measurements interestingly show the presence of hydrous and anhydrous forms of calcium carbonate in samples. Hydrated calcium carbonates include ikaite (calcium carbonate hexahydrate, $\text{CaCO}_3 \cdot 6\text{H}_2\text{O}$) and $\text{CaCO}_3 \cdot \text{H}_2\text{O}$ (calcium carbonate monohydrate). These compounds can exist in a hydrous state for a short time only, as they are metastable in solution under ordinary temperature and pressure conditions (e.g. Marland, 1975; Tlili et al., 2001). In particular, ikaite is stable in solution only at low temperatures, and under a pressure of 1 atm at +3 °C it starts to dehydrate spontaneously after 1 h (Tlili et al., 2001). Ikaite therefore rapidly transforms into monohydrocalcite or anhydrous calcium carbonate and water when the temperature increases at ambient conditions. The decrease in time of the microparticle volume (mass) after melting of the ice can therefore be reasonably ascribed to the spontaneous dehydration of hydrous calcium carbonate and its subsequent solubilization in a slightly acid environment.

4.2. Hydrated calcium carbonates and the role of transport

As far as the geographic provenance of dust particles in the Ross Sea coastal area is concerned, there are as yet no geochemical measurements on dust in snow and firn. In principle, one can arguably assume a long-range provenance of dust, as in the case of the sites located in the interior, where South America was likely the dominant dust supplier during the Late Quaternary glacial stages (Basile et al., 1997; Delmonte et al., 2004), whereas different sources contributed during interglacials (Revel-Rolland et al., 2006; Delmonte et al., 2007). Maggi and Petit (1998) suggested that additional dust inputs from active local (Antarctic) sources, including e.g. non-glaciated areas of coastal Antarctica, sedimentary deposits occurring at glacier margins or weathered outcropping rocks, should also be taken into account for coastal sites. In our samples, the relatively high abundance of calcium carbonates, which are absent or negligible in the plateau ice cores (DeAngelis et al., 1992; Delmonte et al., 2004; Marino et al., 2004) and in the local rock outcrops (Ricci, 1997 and references therein), points to another very productive source of carbonates. The presence of ikaite, a mineral formed in cold waters under rather specific conditions and the first mineral to precipitate in the brine layer on top of newly formed sea ice at temperatures below -2.2 °C (e.g. Thompson and Nelson, 1956; Assur, 1960; Papadimitriou et al., 2003; Eicken, 2003; Sander et al., 2006 and references therein), provides clues about the carbonate source. We suggest that ikaite, monohydrocalcite and the carbonates we find in our samples are primary aerosols deflated from the surface of sea ice forming during winter in front of our coastal drilling sites, and covering a vast surface area. Note that the observed hydrous carbonates are different from the secondary aerosol phases produced in the atmosphere or ice layers, e.g. the sulphate salts observed in ice from inland sites of Antarctica such as Dome Fuji (e.g. Ohno et al., 2005; Iizuka et al., 2006).

As we assume that hydrous calcium carbonates are primary aerosols coming from sea ice, then the presence in the firn of calcium carbonates must be related to the atmospheric transport of aerosols and to the cyclonic activity at the sea ice edge, which likely favours mobilization and transport of sea ice salts. All these factors vary on seasonal and interannual timescales, as wind patterns and the spatial distribution of cyclones around the Antarctic are linked to a number of meteo-climatic factors (King and Turner, 1997; Simmonds, 2003; White et al., 2004; White and Simmonds, 2006).

The investigated drilling sites are located at the convergence of very cold air masses (katabatic winds) blowing from the Antarctic inland (Frezzotti et al., 2007) and milder maritime air masses from lower latitudes (e.g. Parish and Bromwich, 1987). From a palaeoclimatic point of view, isotopic and chemical records from the TD core, drilled in the framework of the 1995/1996 IT-ITASE traverse, indicate that maritime air mass intrusions have played a significant role in the area over the last 800 yr (Stenni et al., 2002; Proposito et al., 2002; Becagli et al., 2004).

Air travelling at high altitudes (4000 m above Talos Dome) mainly originates from the Antarctic Plateau (~20%) and the Indian (~40%) and Pacific (~20%) oceans. About 40% of these trajectories travel over the plateau, whereas a minor fraction (~20%) essentially travels over the Indian Ocean (Scarchilli, 2007). Conversely, low altitude trajectories (ca. 1000 m above Talos Dome) are much more influenced by topography. About 50% of these originate from the Antarctic interior, whereas about 30% come from the Ross Sea. We tested the occurrence and frequency of air mass trajectories capable of transporting particles from the sea ice surface to Talos Dome using the HYSPLIT (HYbrid Single-Particle Lagrangian Integrated Trajectory) model (Draxler and Rolph, 2003). We first calculated a set of 2-day back trajectories for every day from 01/02/1990 to 01/02/2002, selecting a starting point 1000 m above Talos Dome and using the ECMWF Re-Analysis ERA-40 data field as the input meteorological dataset. We then considered only air mass trajectories travelling through the mixed layer over a region where the ice cover value is greater than 0.5% and surface wind speeds are greater than 8 m/s (Berthier et al., 2006) during fall, winter and spring. In the examined twelve-year period (1990–2002), there are episodes of favourable conditions for particle transport from the sea ice over the continent. The number of favourable events in the investigated period varies from 1 to 10, with an average of 6. This means that this type of events is rare but likely. Seasonal analysis revealed that the trajectories of favourable events mainly come from the Ross Sea during fall and spring and from the Southern and Indian Ocean sectors during winter (Fig. 7).

4.3. A two-century dust record from the Talos Dome region

The decrease in total microparticle volume (mass) through time after sample melting is related to dehydration and solubilization of hydrous calcium carbonates. Although the physical mechanisms have still to be assessed, we assume these compounds could originate from the surface of sea ice. In this hypothesis, cyclonic activity plays a major role, enhancing their mobilization and transport to the drilling sites. The total (t_0) dust concentration therefore represents the cumulative contribution of soluble and insoluble dust, whereas the concentration after 24 h (t_{24}) represents the insoluble component alone (Fig. 5a).

The insoluble dust concentration record from the TDC core shows interesting decadal-scale oscillations which are particularly marked during the 20th century. Interestingly, the insoluble dust concentration record shows a marked increase around 1930, a feature already observed by Maggi and Petit (1998) in the Hercules Nevé (NVL, 73°06'S, 165°27'E) firn core and attributed to a general increase in atmospheric dustiness related to a period of pronounced aridity in the Southern Hemisphere and likely the world over.

Comparison between the TDC soluble dust record and the mean (March to November) 500 mbar geopotential height (60–70°S; 150–200°E, see Fig. 5b and c) suggests that sea ice-derived salts are likely associated with enhanced cyclonic conditions.

5. Conclusions

We observed in this work the presence of soluble hydrated carbonates in coastal firn cores from the Northern Victoria Land. The presence of mono- and hexa-hydrate calcium carbonates, in particular, suggests a possible provenance of these compounds from the sea ice surface. Much work is needed in the future for the assessment of the physical mechanisms leading to mobilization and transport of these salts.

The new deep ice core currently being drilled at Talos Dome in the framework of the TALDICE Project will hopefully extend mineralogical evidence observed in the TDC soluble dust record, presented in this work, to the entire last climatic cycle.

Acknowledgements

Research was carried out in the framework of the Project on Glaciology of the *Programma Nazionale di Ricerche in Antartide* (PNRA)-MIUR and financially supported by the PNRA Consortium through collaboration with ENEA Roma. This work is an Italian contribution to the ITASE project. Talos Dome Ice core Project (TALDICE), a joint European programme, funded by national contributions from Italy, France, Germany, Switzerland and the United Kingdom. The main logistic support was provided by PNRA. This is a TALDICE publication no 2.

References

- Assur, A., 1960. Composition of sea ice and its tensile strength. CRREL Res. Rep. 44.
- Basile, I., Grousset, F.E., Revel, M., Petit, J.R., Biscaye, P.E., Barkov, N.I., 1997. Patagonian origin of glacial dust deposited in East Antarctica (Vostok and Dome C) during glacial stages 2, 4 and 6. *Earth Planet. Sci. Lett.* 146, 573–589.
- Becagli, S., Benassai, S., Castellano, E., Largiuni, O., Migliori, A., Traversi, R., Flora, O., Udisti, R., 2004. Chemical characterization of the last 250 years of snow deposition at Talos Dome (East Antarctica). *Int. J. Environ. Anal. Chem.* 84 (6–7), 523–536.
- Berthier, S., Chazette, P., Couvert, P., Pelon, J., Dulac, F., Thieuleux, F., Moulin, C., Pain, T., 2006. Desert dust aerosol columnar properties over ocean and continental Africa from Lidar in-Space Technology Experiment (LITE) and Meteosat synergy. *J. Geophys. Res.* 111 (D21), D21202. doi:10.1029/2005JD006999.
- Briat, M., Royer, A., Petit, J.R., Lorius, C., 1982. Late glacial input of eolian continental dust in the Dome C ice core: additional evidence from individual microparticle analysis. *Ann. Glaciol.* 3, 27–30.
- Clarkson, J.R., Price, T.J., Adams, C.J., 1992. *J. Chem. Soc., Faraday Trans.* 88, 243.
- Coleyshaw, E.E., Crump, G., Griffith, W.P., 2003. Vibrational spectra of the hydrated carbonate minerals ikaite, monohydrocalcite, lansfordite and nesquehonite. *Spectrochim. Acta A Mol. Biomol. Spectrosc.* 59 (10), 2231–2239.
- Dahl, K., Buchard, B., 2006. Monohydrocalcite in the Arctic Ikka Fjord, SW Greenland: first reported marine occurrence. *J. Sediment. Res.* 76, 460–471. doi:10.2110/jgsr.2006.035.
- Dapiaggi, M., Sala, M., Artioli, G., Fransen, M.J., 2007. Evaluation of the phase detection limit on filter-deposited dust particles from Antarctic ice cores. *Zeitschrift für Kristallographie, Kristallogr. Suppl.* 26, 73–78.
- DeAngelis, M., Barkov, N.I., Petrov, V.N., 1992. Sources of continental dust over Antarctica during the last glacial cycle. *J. Atmos. Chem.* 14, 233–244.
- Delmonte, B., Petit, J.R., Maggi, V., 2002. Glacial to Holocene implications of the new 27000-year dust record from the EPICA Dome C (East Antarctica) ice core. *Clim. Dyn.* 18 (8), 647–660.
- Delmonte, B., Basile-Doelsch, I., Petit, J.R., Maggi, V., Revel-Rolland, M., Michard, A., Jagoutz, E., Grousset, F., 2004. Comparing the Epica and Vostok dust records during the last 220,000 years: stratigraphical correlation and provenance in glacial periods. *Earth Sci. Rev.* 66, 63–87.
- Delmonte, B., Petit, J.R., Krinner, G., Maggi, V., Jouzel, J., Udisti, R., 2005. Ice core evidence for secular variability and 200-year dipolar oscillations in atmospheric circulation over East Antarctica during the Holocene. *Clim. Dyn.* 24 (6), 641–654.
- Delmonte, B., Petit, J.R., Basile-Doelsch, I., Jagoutz, E., Maggi, V., 2007. Late Quaternary Interlacials in East Antarctica from ice core dust records. Book chapter In: Sirocko, F., Litt, T., Claussen, M. (Eds.), *The Climate of Past Interglacials*. ELSEVIER, pp. 53–73.
- Draxler, R.R., Rolph, G.D., 2003. HYSPLIT (HYbrid Single-Particle Lagrangian Integrated Trajectory model) model. NOAA AIR RESOUR. LAB., Silver Spring, MD. <http://www.arl.noaa.gov/ready/hysplit4.html>.
- Durst, R.A., Davison, W., Koch, W.F., 1994. Recommendations for the electrometric determination of the pH of atmospheric wet deposition (acid rain). *Pure Appl. Chem.* 66 (3), 649–658.
- Eicken, H., 2003. From microscopic, to the macroscopic, to regional scale: growth, microstructure and properties of sea ice. In: Thomas, D.N., Dieckmann, G.S. (Eds.), *Sea Ice. An Introduction to its Physics, Chemistry, Biology and Geology*. Blackwell, Oxford, UK, pp. 22–81.
- EPICA community members, 2004. Eight glacial cycles from an Antarctic ice core. *Nature* 429, 623–628.
- Frezzotti, M., Flora, O., 2002. Ice dynamic features and climatic surface parameters in East Antarctica from Terra Nova Bay to Talos Dome and Dome C: ITASE Italian traverses. *Terra Antarctica* 9, 47–54.
- Frezzotti, M., Bitelli, G., de Michelis, P., Deponti, A., Forieri, A., Gandolfi, S., Maggi, V., Mancini, F., Rémy, F., Tabacco, I.E., Urbini, S., Vittuari, L., Zirizzotti, A., 2004a. Geophysical survey at Talos Dôme (East Antarctica): the search for a new deep-drilling site. *Ann. Glaciol.* 39, 423–432.
- Frezzotti, M., Pourchet, M., Flora, O., Gandolfi, S., Gay, M., Urbini, S., Vincent, C., Becagli, S., Gragnani, R., Proposito, M., Severi, M., Traversi, R., Udisti, R., Fily, M., 2004b. New estimations of precipitation and surface sublimation in East Antarctica from snow accumulation measurements. *Clim. Dyn.* 23 (7–8), 803–813.
- Frezzotti, M., Pourchet, M., Flora, O., Gandolfi, S., Gay, M., Urbini, S., Vincent, C., Becagli, S., Gragnani, R., Proposito, M., Severi, M., Traversi, R., Udisti, R., Fily, M., 2005. Spatial and temporal variability of snow accumulation in East Antarctica from traverse data. *J. Glaciol.* 51 (172), 113–124.
- Frezzotti, M., Urbini, S., Proposito, M., Scarchilli, C., Gandolfi, S., 2007. Spatial and temporal variability of surface mass balance near Talos Dome, East Antarctica. *J. Geophys. Res.* 112 (F02032). doi:10.1029/2006JF000638.
- Gaudichet, A., Petit, J.R., Lefevre, R., Lorius, C., 1986. An investigation by analytical transmission electron microscopy of individual insoluble microparticles from Antarctic (Dome C) ice core samples. *Tellus* 38B, 250–261.
- Gaudichet, A., Angelis, M.D., Lefevre, R., Petit, J.R., Korotkevitch, Y.S., Petrov, V.N., 1988. Mineralogy of insoluble particles in the Vostok Antarctic ice core over the last climatic cycle (150 kyr). *Geophys. Res. Lett.* 15 (13), 1471–1474.
- Gaudichet, A., De Angelis, M., Joussaume, S., Petit, J.R., Korotkevitch, Y.S., Petrov, V.N., 1992. Comments on the origin of dust in East Antarctica for present and ice age conditions. *Atmos. Chem.* 14, 129–142.
- Iizuka, Y., Hondoh, T., Fuji, Y., 2006. Na₂SO₄ and MgSO₄ salts during the Holocene period derived by high-resolution depth analysis of Dome Fuji ice core. *J. Glaciol.* 52, 58–64.
- King, J.C., Turner, J., 1997. *Antarctic Meteorology and Climatology*. Cambridge University press.
- Maggi, V., 1997. Mineralogy of atmospheric microparticles along the Greenland Ice Core Project ice core. *J. Geophys. Res.* 102 (C12), 26725–26734.
- Maggi, V., Petit, J.R., 1998. Atmospheric dust concentration record from the Hercules Nève ice core, northern Victoria Land, Antarctica. *Ann. Glaciol.* 27, 355–359.
- Marino, F., Maggi, V., Delmonte, B., Ghermandi, G., Petit, J.R., 2004. Elemental composition (Si, Fe, Ti) of atmospheric dust over the last 220 kyr from the EPICA ice core (Dome C, Antarctica). *Ann. Glaciol.* 39, 110–118.
- Marino, F., Calzolari, G., Caporali, S., Castellano, E., Chiari, M., Lucarelli, F., Maggi, V., Nava, S., Sala, M., Udisti, R., in press. PIXE and PIGE techniques for the analysis of Antarctic ice dust and continental sediments. *Nucl. Instrum. Methods Phys. Res., B Beam Interact. Mater. Atoms*. doi:10.1016/j.nimb.2008.03.029.
- Marland, G., 1975. The stability of CaCO₃·6H₂O (ikaite). *Geochim. Cosmochim. Acta* 39 (1), 83–91.
- Minceva-Sukarova, B., Sherman, W.F., Wilkinson, G.R., 1984. The Raman spectra of ice (I_h, II, III, V, VI and IX) as functions of pressure and temperature. *J. Phys. C. Solid State Phys.* 17, 5833–5850. doi:10.1088/0022-3719/17/32/017.
- NGRIP Project members, 2004. High-resolution record of Northern Hemisphere climate extending into the last interglacial period. *Nature* 431, 147–151.
- Ohno, H., Igarashi, M., Hondoh, T., 2005. Salt inclusions in polar ice core: location and chemical form of water-soluble impurities. *Earth Planet. Sci. Lett.* 232 (1–2), 171–178.
- Papadimitriou, S., Kennedy, H., Kattner, G., Dieckmann, G.S., Thomas, D.N., 2003. Experimental evidence for carbonate precipitation and CO₂ degassing during sea ice formation. *Geochim. Cosmochim. Acta* 68, 1749–1761.
- Parish, T.R., Bromwich, D.H., 1987. The surface windfield over the Antarctic ice sheets. *Nature* 328, 51–54.
- Pauly, H., 1963. Ikaite, a new mineral from Greenland. *Arctic* 16.
- Petit, J.R., Jouzel, J., Raynaud, D., Barkov, N.I., Barnola, J.M., Basile, I., Bender, M., Chappellaz, J., Davis, M., Delaygue, G., Delmotte, M., Kotlyakov, V.M., Legrand, M., Lipenkov, V.Y., Lorius, C., Pépin, L., Ritz, C., Saltzman, E., Stievenard, M., 1999. Climate and atmospheric history of the past 420,000 years from the Vostok ice core, Antarctica. *Nature* 399, 429–436. doi:10.1038/20859.
- Proposito, M., Becagli, S., Castellano, E., Flora, O., Genoni, L., Gragnani, R., Stenni, B., Traversi, R., Udisti, R., Frezzotti, M., 2002. Chemical and isotopic snow variability along the 1998 ITASE traverse from Terra Nova Bay to Dome C (East-Antarctica). *Ann. Glaciol.* 35, 187–194.
- Revel-Rolland, M., De Deckker, P., Delmonte, B., Hesse, P.P., Magee, J.W., Basile-Doelsch, I., Grousset, F., Bosch, D., 2006. Eastern Australia: a possible source of dust in East Antarctica interglacial ice. *Earth Planet. Sci. Lett.* 249 (1–2), 1–13.
- Ricci, C.A., 1997. *The Antarctic Region: Geological Evolution and Processes*. Terra Antarctica Publications.
- Sander, R., Burrows, J., Kaleschke, L., 2006. Carbonate precipitation in brine – the trigger for tropospheric ozone depletion events. *Atmos. Chem. Phys.* 6, 4653–4658.
- Scarchilli, C., 2007. *Precipitation and sublimation impact on snow accumulation over Antarctica*. Ph.D. thesis, University of Siena, Siena, Italy, in preparation.
- Simmonds, I., 2003. Modes of atmospheric variability over the Southern Ocean. *J. Geophys. Res. (Ocean)* 108 (C4), SOV 5–1. doi:10.1029/2000JC000542 ID 8078.
- Stenni, B., Proposito, M., Gragnani, R., Flora, O., Jouzel, J., Falourd, S., Frezzotti, M., 2002. Eight centuries of volcanic signal and climate change at Talos Dome (East Antarctica). *J. Geophys. Res.* 107 (D9). doi:10.1029/2000JD000317.
- Thompson, T.G., Nelson, K.H., 1956. Concentration of brines and deposition of salts from sea water under frigid conditions. *Am. J. Sci.* 254, 227–238.
- Tlili, M.M., Ben Amor, M., Gabrielli, C., Joiret, S., Maurin, G., Rousseau, P., 2001. Characterization of CaCO₃ hydrates by micro-Raman spectroscopy. *J. Raman Spectrosc.* 33, 10–16.
- Watanabe, O., Jouzel, J., Johnsen, S., Parrenin, F., Shoji, H., Yoshida, N., 2003. Homogeneous climate variability across East Antarctica over the past three glacial cycles. *Nature* 422, 509–512.
- White, W.B., Simmonds, I., 2006. Sea surface temperature-induced cyclogenesis in the Antarctic circumpolar wave. *J. Geophys. Res.* 111 (C08011). doi:10.1029/2004JC002395.
- White, W.B., Gloersen, P., Simmonds, I., 2004. Troposphere response in the Antarctic circumpolar wave along the sea ice edge around Antarctica. *J. Climate* 17, 2765–2779.